

Definition of Hepatic Tumor Microcirculation by Single Photon Emission Computerized Tomography (SPECT)

John W. Gyves, Harvey A. Ziessman, William D. Ensminger, James H. Thrall, John E. Niederhuber, John W. Keyes, Jr.,
and Suzette Walker

University of Michigan Medical Center, Ann Arbor, and Henry Ford Hospital, Detroit, Michigan

Single photon emission computerized tomography coupled with Tc-99m MAA hepatic-arterial perfusion scintigraphy has been used to examine the density of the functional microcirculation of hepatic tumors relative to normal liver in 24 patients. In both colorectal and carcinoid tumors we have demonstrated an average three-fold greater arteriolar-capillary density in areas of tumor proliferation. The depth of the evoked tumor hypervascularity was found to extend about 4 cm. Tumors greater than 8–9 cm in diameter were uniformly found to have a central hypovascular core. These observations are of importance in the design of selective strategies utilizing therapeutic microspheres directed against the hypervascular proliferating regions of human tumors.

J Nucl Med 25: 972–977, 1984

Tumors must have adequate nutrition to grow and, therefore, much effort has been devoted to clarify the factors that generate the tumor neovascularity essential to continued tumor growth (1,2). The techniques of radionuclide intraarterial perfusion scintigraphy (3–4) and single photon emission computerized tomography (SPECT) (5) provide tools for quantifying differences between tumor and normal tissue microvasculature.

Radionuclide studies using Tc-99m macroaggregated albumin (Tc-99m MAA) have used hepatic arterial injection to determine drug distribution at the low flow rates used during intraarterial chemotherapy (3–4). These albumin particles average 30–40 μm in diameter (range of 10–90 μm) and are held in the first arteriolar-capillary bed encountered. It is this level of the circulation that presumably supplies nutrient vessels for continued tumor growth. Assuming homogeneous mixing in the hepatic artery, the relative Tc-99m MAA activity in the liver should directly reflect the relative

density of the microvasculature patency at the time of injection. Thus SPECT coupled with radionuclide perfusion imaging has enabled us to examine in vivo the density of the functional hepatic tumor microcirculation compared with that in normal liver. The availability of a patient population with liver cancers, treated with a totally implanted hepatic arterial drug-delivery system (6), has afforded the opportunity to examine the hepatic tumor microcirculation in the most relevant setting.

METHODS

Twenty-four patients with biopsy-proven, unresectable primary or metastatic liver tumors (Table 1) underwent surgical placement of a silastic catheter and infusion pump for hepatic arterial chemotherapy, as previously described (6). All patients had measurable disease by technetium-99m sulfur colloid (Tc-99m SC) liver-spleen study.

Six mCi of Tc-99m MAA in 0.5–1.0 cc saline were injected slowly over 1 min through the pump sideport into the hepatic artery catheter and then flushed with saline. Conventional planar images with 1000k counts

Received Dec. 23, 1983; revision accepted Apr. 6, 1984.

For reprints contact: John W. Gyves, MD, Upjohn Center for Clinical Pharmacology, University of Michigan Medical Center, Ann Arbor, Michigan. 48109.

TABLE 1. PATIENT CHARACTERISTICS

Diagnosis	
Colorectal Cancer	18
Carcinoid tumor	5
Hepatoma	1
	<hr/> 24
Sex	
Male	10
Female	14
Age (years)	
Range	32-73
Median	58
Mean	57.4

of the liver were acquired in the anterior, posterior, right lateral and left lateral projections. A wide-field-of-view gamma camera with a high-resolution, parallel-hole collimator was used, interfaced to a computer. Fifteen-second images were then obtained from 64 equally spaced projections rotating about the patient's body in a 360° arc. Transaxial tomographic images (1.875 cm thick) were reconstructed using filtered back-projection algorithms and a modified-ramp Hanning 0.5 smoothing filter. In each case enough slices were obtained to encompass the entire liver. We analyzed only those lesions that could be separated from adjacent normal liver and not obscured by other lesions. Thus, only discrete lesions were studied. Attenuation correction was performed using proprietary software with an algorithm based on the assumption of uniform attenuation.

The ratios between the Tc-99m MAA entrapment (and thus blood flow) in the center and the periphery of a tumor nodule and that in the adjacent uninvolved liver were obtained from profile histograms through the center of each discretely identifiable lesion (Fig. 3). The orientation of the profile histogram was selected to encompass a portion of normal liver on either side of the individual lesion. The maximal count density in perfused

portions of tumors was compared with the maximum in uninvolved liver tissue immediately adjacent to the metastatic lesions. Therefore, the perfusion to the vascular portions of the tumor relative to uninvolved liver is denoted by the ratio of count densities from these respective regions. Tumor nodule size was determined using the profile histogram by measuring the maximum diameter of the nodule and width of one hypervascular rim when present.

RESULTS

Figure 1 shows tomographic transaxial slices of a liver-spleen image using Tc-99m sulfur colloid (Tc-99m SC) (A) and a comparable tomographic image after hepatic-arterial injection of Tc-99m MAA (B). These images were obtained 48 hr apart. The large photon-deficient area in the central portion of the liver-spleen image (Fig. 1A) in a patient with proven metastatic colon cancer is seen to have a rim of increased activity on the Tc-99m MAA perfusion study (Fig. 1B). This rim is at the periphery but within the boundaries of the metastatic lesion defined by Tc-99m SC image. The rim shows more Tc-99m MAA activity than the surrounding normal liver, which is only faintly imaged. The central portion of this large nodule contains relatively less Tc-99m MAA activity. Figure 2 shows the profile histogram of the nodule in Fig. 1. The relative Tc-99m MAA activities in the rim, central core, and surrounding normal liver were calculated from ratios of count densities in these areas.

Twenty-six liver tumor nodules were analyzed in 18 patients with biopsy-proven metastatic colon cancer (Table 2). These nodules have been ranked according to increasing diameter. Nodules ≥ 9.5 cm in diameter appear to have a central portion that fails to show any evidence of Tc-99m MAA entrapment. The size of the hypovascular core is somewhat variable but in all cases the core is surrounded by a rim of increased Tc-99m MAA activity. The size of this rim is less variable compared with the core, with a median of 3.2 cm (range

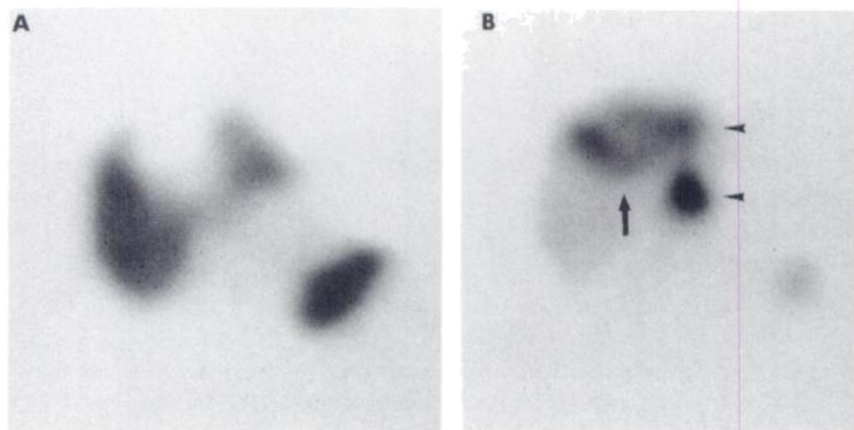


FIG. 1. A: Transaxial tomographic section through Tc-99m SC liver-spleen scintigram, showing large focal defect in patient with proven metastatic colon cancer. **B:** Comparable transaxial tomographic slice after hepatic-arterial infusion of Tc-99m MAA, showing rim of increased activity at periphery of metastatic nodule (\leftarrow). There is also extrahepatic perfusion to stomach (\leftarrow).

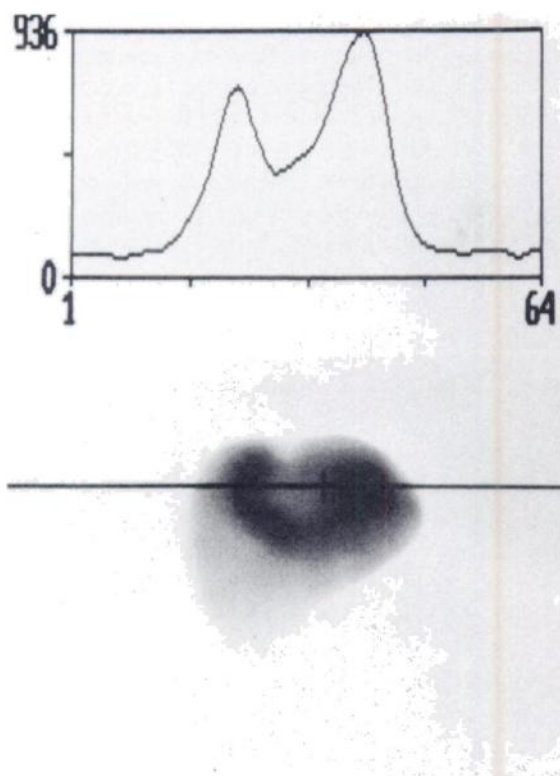


FIG. 2. Profile histogram of tumor nodule in Fig. 1B. Counts are displayed on vertical axis, and pixels on horizontal axis. Count ratio was determined by using lateral rim and adjacent liver.

1.8–4.2 cm). In contrast, nodules <8.5 cm in diameter fail to show any evidence of a hypovascular core, and thus appear solid. Using the Wilcoxon two-sample rank sum test, the size dependency of the presence or absence of a hypovascular core is found highly significant ($p < 0.0005$) (7). The greatest rim thickness in the ten largest nodules with diameters >9.5 cm was 4.2 cm. The maximum radius of the small solid nodules was 4.2 cm, probably indicating that the maximum depth to which tumor neovascularity can be generated from surrounding normal liver is approximately 4 cm. Table 2 also presents the relative Tc-99m MAA activity in areas of tumor, compared with normal liver. In these patients the ratio was always greater than 1 (median 2.7) and was unrelated to nodule size.

Table 3 presents similar data for 14 carcinoid tumor nodules in five patients. Large nodules with diameters >8.9 cm had a central core lacking Tc-99m MAA activity, but always retained a rim of increased Tc-99m MAA activity. Nodules less than 8 cm failed to show any evidence of a central core and thus appeared solid. The Wilcoxon test demonstrated the size dependency of the presence or absence of a hypovascular core to be highly significant ($p < 0.001$). The largest rim thickness among the six large nodules with diameters >8.9 cm was 3.9 cm (median 3.3 cm), which approximated the radius of the largest solid nodule. The ratio of Tc-99m MAA activity

in carcinoid tumors relative to normal liver was again greater than 1 (median 4.4).

Three small nodules (4.2, 6.0, and 6.6 cm in diameter) were examined in a single patient with hepatocellular carcinoma. These nodules all had a solid vascular pattern by Tc-99m MAA imaging as described above for colorectal and carcinoid hepatic metastases. There was a marked increase in radioactivity in these nodules relative to surrounding normal liver. In this patient the ratio of radioactivity in areas of tumor was 20–30 times that in surrounding normal liver. This suggests that the microcirculation density of hepatocellular carcinoma nodules may be greater than in either metastatic colon cancer or carcinoid tumor nodules, although additional patients will need to be studied.

DISCUSSION

The description of tumors as hypovascular or hypervascular relative to normal liver, based upon their contrast angiographic appearance (9,10), may mask important vascular distribution differences that can be quantified by the more sensitive modality of SPECT. The Tc-labeled macroaggregated particles used in this study are trapped at the level of the arteriolar-capillary

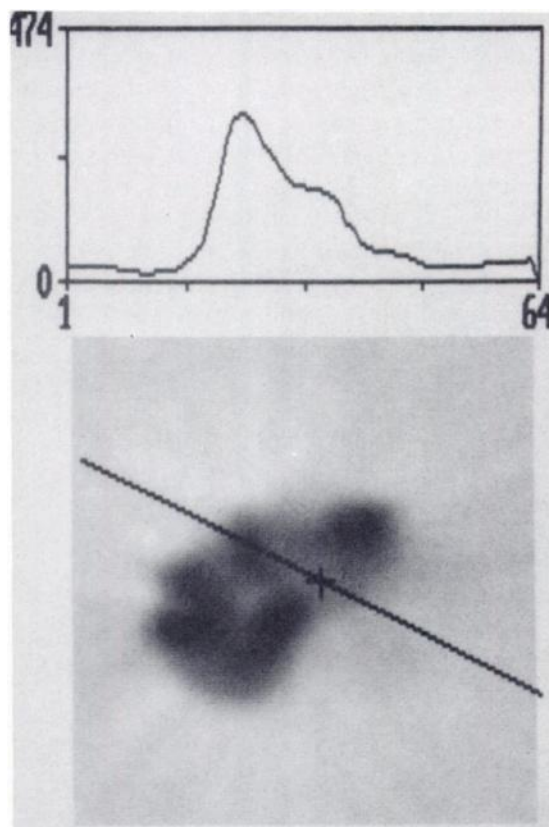


FIG. 3. Profile histogram through solid tumor nodule and adjacent liver. The Tc-MAA tumor-to-liver count ratio was determined by comparing maximal count density of tumor nodule with count density in adjacent uninvolved liver tissue.

**TABLE 2. COLON CANCER TUMOR NODULES
HEPATIC TUMOR AND LIVER MICROCIRCULATORY VASCULARITY DETERMINED BY SPECT**

Lesion No.	Diameter (cm)	Hypovascular core (cm)	Tumor vascularity (cm)	Tc MAA cpm ratios: tumor/normal liver
1	2.4	None	Solid	4.6
2	2.4	None	Solid	4.1
3	2.4	None	Solid	2.5
4	2.4	None	Solid	2.5
5	3.0	None	Solid	1.3
6	3.0	None	Solid	3.4
7	3.6	None	Solid	2.7
8	4.2	None	Solid	1.8
9	4.2	None	Solid	2.5
10	4.8	None	Solid	2.6
11	4.8	None	Solid	2.3
12	5.4	None	Solid	2.1
13	5.4	None	Solid	5.4
14	6.6	None	Solid	6.4
15	6.6	None	Solid	1.2
16	8.4	None	Solid	3.4
17	9.6	2.4	Rim (3.6)	4.6
18	10.2	3.0	Rim (3.6)	8.0
19	10.2	3.6	Rim (3.3)	2.3
20	10.2	7.2	Rim (1.8)	3.9
21	10.2	5.4	Rim (2.4)	4.5
22	11.4	5.4	Rim (3.0)	5.3
23	12.0	6.6	Rim (3.0)	2.3
24	12.6	4.2	Rim (4.2)	2.5
25	13.2	9.0	Rim (3.0)	1.8
26	16.8	8.4	Rim (3.6)	2.7

bed and thus permit evaluation of the nutrient vessels involved in the proliferating portions of tumor nodules.

There have been several attempts to quantify the perfusion and blood flow in experimental metastatic tumors in the liver. The perfusion of Walker carcino-

**TABLE 3. CARCINOID TUMOR NODULES
HEPATIC TUMOR AND LIVER MICROCIRCULATORY VASCULARITY DETERMINED BY SPECT**

Lesion No.	Diameter (cm)	Hypovascular core (cm)	Tumor vascularity (cm)	Tc MAA cpm ratios: tumor/normal liver
1	2.4	None	Solid	6.0
2	3.0	None	Solid	3.5
3	3.0	None	Solid	4.5
4	3.6	None	Solid	1.4
5	4.2	None	Solid	8.7
6	7.2	None	Solid	4.7
7	7.2	None	Solid	1.6
8	7.8	None	Solid	1.8
9	9.0	2.4	Rim (3.0)	3.2
10	9.6	1.8	Rim (3.9)	4.3
11	9.6	4.8	Rim (2.4)	5.6
12	11.4	4.2	Rim (3.6)	5.1
13	15.0	7.8	Rim (2.4)	6.1
14	17.4	10.2	Rim (3.6)	3.2

sarcoma implants in the livers of rats has been studied by Ackerman et al. (17). Radioactivity in liver specimens excised immediately after injection of radioiodinated serum albumin into the arterial system was measured. In large tumors, the mean tumor-to-liver radioactivity ratio was 7.2 ± 2.3 (median 3.0). When yttrium-90-labeled microspheres (mean $86 \mu\text{m}$) were injected into the hepatic artery in the same animal model, the mean tumor-to-liver activity ratio was 2.4 ± 0.3 (mean 1.9) (17). Similar studies using radioactive microspheres $15 \mu\text{m}$ in diameter have been done in Walker tumors in rats (18) and VX₂ tumors in rabbits (19), with reported mean tumor-to-liver ratios of 4.8 and 4.2, respectively.

The results reported here for human tumor nodules, studied in vivo by SPECT, are consistent with, and expand upon, findings reported in animal systems. Hepatic tumor nodules from both colorectal cancer and carcinoid are hypervascular compared with adjacent uninvolved liver, and the pattern of hypervascularity is dependent on tumor size. Large nodules possess a central portion that is relatively hypovascular, whereas smaller nodules are uniformly hypervascular. In both colorectal and carcinoid tumors, the density of this microvasculature is approximately three times that of surrounding normal liver. Due to technical limitations in SPECT imaging, count ratios for small structures may be underestimated. Hoffman et al. have shown that this error could be as much as a factor of 2 (21). Therefore the relative magnitude of activity ratios should be a conservative estimate.

Thus, both metastatic carcinoid and colorectal cancer are hypervascular by this assessment. Although colon-tumor nodules metastatic to the liver have usually been described as hypovascular on celiac angiography, recent studies using superselective hepatic angiographic techniques have shown that nearly all hepatic metastases are hypervascular (8).

In the current studies the maximum depth of this neovascular growth appears to be about 4 cm. In tumor nodules >8 cm in diameter the current technique consistently demonstrates a central hypovascular core that correlates pathologically with the often recognized necrotic center seen in large tumors. Although the SPECT system used in this study is limited by its resolution (18–20 mm FWHM), Jaszczak et al., using a comparable system, were able to detect photon-deficient areas as small as 1 cm in diameter within a liver-sized object (20). This implies that the uniform appearance of a hypovascular core within lesions >8 cm diam is a real phenomenon, not artifact. However, the apparent size of this central core and tumor nodule may be somewhat dependent on the activity ratio. A focus of greatly increased uptake (high tumor-to-normal-liver ratio) may appear larger in overall size, with a smaller apparent central core, than a tumor nodule of the same size with a lower activity ratio.

Our observations suggest that potentially exploitable differences between normal liver and hepatic tumor microcirculation exist, and may ultimately enhance the potency of regional chemotherapy. The availability of reliable infusion systems (6,12) and the technology to monitor therapy (3–4) allow repeated reliable access to the hepatic arterial watershed and tumor within the liver. With the information presented above, therapeutic potency may be increased by efforts to focus therapy on the hypervascular portions of tumor, where presumably active tumor proliferation takes place.

Currently, the intraarterial administration of biodegradable starch microspheres in conjunction with cytotoxic agents is undergoing study (13,14), and yttrium-90 radioactive resin microspheres have been used clinically for intraarterial radiotherapy (15). The hepatic-arterial administration of radioactive microspheres, or a suspension of starch microspheres in an appropriate drug solution, results in improved delivery of the therapeutic agent to the tumor's microcirculation relative to normal liver. Under these circumstances, delivery of the internal radiation or drug solution within the tissue should be proportional to the microcirculation volume, which is in turn proportional to the activity of the Tc-99m MAA entrapped in a given region of the tissue. Clinical studies utilizing therapeutic microspheres and taking advantage of this selectivity may improve the therapy of hepatic tumors. In addition, studies in animal models and in humans suggest that certain pharmacologic agents (i.e., vasoconstrictors) may result in a shift of blood flow away from normal liver and toward tumor (11). SPECT, in conjunction with Tc-99m MAA hepatic arterial perfusion scintigraphy, provides a means of studying and quantifying these perfusion changes in vivo.

ACKNOWLEDGMENTS

Supported in part by grants CA33825 and 5-MO-1-RR-42 from the National Institutes of Health, the Burroughs Wellcome Fund and The American Cancer Society.

REFERENCES

1. FOLKMAN J: Tumor angiogenesis: Therapeutic implications. *N Engl J Med* 285:1182–1186, 1971
2. FOLKMAN J: Tumor Angiogenesis. In *A Comprehensive Treatise Vol 3 Biology of Tumors: Cellular Biology and Growth*. Becker FF, ed. New York, Plenum Publishing Corp., pp 355–388, 1975
3. KAPLAN WD, ENSMINGER WD, COME SE, et al: Radio-nuclide angiography to predict patient response to hepatic artery chemotherapy. *Cancer Treat Rep* 64:1217–1222, 1980
4. YANG PJ, THRALL JH, ENSMINGER WD, et al: Perfusion scintigraphy (Tc-99m MAA) during surgery for placement of chemotherapy catheter in hepatic artery; Concise communication. *J Nucl Med* 23:1066–1069, 1982
5. KEYES JW, ORLANDEA N, HEETDERKS WJ, et al: The

- humongotron—A scintillation-camera transaxial tomograph. *J Nucl Med* 18:381-387, 1977
6. ENSMINGER W, NIEDERHUBER J, DAKHIL S, et al: Totally implanted drug delivery system for hepatic arterial chemotherapy. *Cancer Treat Rep* 65:393-400, 1981
 7. BROWN B, HOLLANDER M: *Statistics: A Biomedical Introduction*. New York, John Wiley and Sons, 1977
 8. CHUANG VP: Hepatic tumor angiography: A subject review. *Radiology* 148:633-639, 1983
 9. HEALEY JE: Vascular pattern in human metastatic liver tumors. *Surg Gynecol Obstet* 120:1187-1193, 1965
 10. REUTER S: The current status of angiography in the evaluation of cancer patients. *Cancer* 37:532-541, 1976
 11. ACKERMAN NB, HECHMER PA, et al.: The blood supply of experimental liver metastases: V. Increased tumor perfusion with epinephrine. *Am J Surg* 140:625-631, 1980
 12. NIEDERHUBER JE, ENSMINGER W, GYVES JW, et al: Totally implanted venous and arterial access system to replace external catheters in cancer treatment. *Surgery* 92:706-712, 1982
 13. DAKHIL S, ENSMINGER W, CHO K, et al: Improved regional selectivity of hepatic arterial BCNU with degradable microspheres. *Cancer* 50:631-635, 1982
 14. GYVES JW, ENSMINGER WD, VANHARKEN D, et al: Improved regional selectivity of hepatic arterial mitomycin by starch microspheres. *Clin Pharm Ther* 34:259-265, 1983
 15. GRADY E: Internal radiation therapy of hepatic cancer. *Dis Col Rect* 22:371-375, 1979
 16. ABRAMS HL: The response of neoplastic renal vessels to epinephrine in man. *Radiology* 82:217-224, 1964
 17. ACKERMAN NB, LIEN WM, KONDI ES, et al: The blood supply of experimental liver metastases: I. The distribution of hepatic artery and portal vein blood to "small" and "large" tumors. *Surgery* 66:1067-1072, 1969
 18. YOUNG SW, HOLLENBERG NK, KAZAM E, et al: Resting host and tumor perfusion as determinants of tumor vascular responses to norepinephrine. *Cancer Res* 39:1898-1903, 1979
 19. BLANCHARD RVW, GROTENHUIS I, LAPAVE JW, et al: Blood supply to hepatic V2 carcinoma implants as measured by radioactive microspheres. *Proc Soc Exp Biol Med* 118:465-468, 1965
 20. JASZCZAK RJ, WHITEHEAD FR, LIM CB: Lesion detection with single-photon emission computed tomography (SPECT) compared with conventional imaging. *J Nucl Med* 23:97-102, 1982
 21. HOFFMAN EJ, HUANG S-C, PHELPS ME: Quantitation in positron emission computed tomography: 1. Effect of object size. *J Comput Assist Tomogr* 3:299-308, 1979

**Southwestern Chapter
Society of Nuclear Medicine
30th Annual Meeting**

March 28-31, 1985

Sheraton New Orleans

New Orleans, Louisiana

Announcement and Call for Abstracts

The Scientific Program Committee of the Southwestern Chapter of the Society of Nuclear Medicine invites submitted abstracts of original work in nuclear medicine from members and nonmembers of the Society of Nuclear Medicine to be considered for the 30th Annual Meeting.

The program will include submitted scientific papers, invited speakers and teaching sessions covering areas of current interest in nuclear medicine. The program will be approved for credit toward the AMA Physicians Recognition Award under Continuing Medical Education Category 1 through the Society of Nuclear Medicine.

Scientific exhibits also are solicited for this meeting. Use the abstract submission guidelines listed below. Descriptions of exhibits, including size, shape and necessary lighting and support requirements should be listed on a separate sheet. Exhibits will be judged on scientific content in the technologist and professional level categories.

The Southwestern Chapter 7th Annual Nuclear Medicine refresher course will be held March 28, 29, 1985. The course will include reviews of basic science, instrumentation, radiopharmaceuticals and in vitro and diagnostic imaging techniques. Nuclear Medicine Scientists, Technologists and Physicians interested in a state of the art review are invited to attend.

Abstract forms may be obtained from:

Southwestern Chapter
1209 Lair Avenue
Metairie, LA 70003
Tel: (504)733-0063

Abstracts must be received in Chapter Office by Dec. 1, 1984 (Postmark).

Additional information may be acquired from:

Richard F. Kieffer, M.D.
7720 Rocking Horse Lane
Boerne, TX 78006
Tel: (512)225-4566